processes

MDPI

Article

Effect of Cobalt- and Nickel-Ion-Modified Zeolite on the Properties of Rubber Compounds

Almira Orazymbetova [1], Guzaliya Sagitova [2,*], Aliya Suigenbayeva [3], Saule Sakibayeva [1], Shaizada Koshkarbayeva [1], Ayaulym Tileuberdi [2,*], Zhadyra Artykova [4], Myrzabay Narmanov [3] and Abdujalol Sidikov [5]

[1] Department of Technology of Inorganic and Petrochemical Industries, M.Auezov South Kazakhstan University, Shymkent 160012, Kazakhstan; almira.oao1976@mail.ru (A.O.); sakibayeva.sayle@mail.ru (S.S.); shayzada-1968@mail.ru (S.K.)
[2] Department of Ecology, M.Auezov South Kazakhstan University, Shymkent 160012, Kazakhstan
[3] Department of Chemistry and Pharmaceutical Engineering, M.Auezov South Kazakhstan University, Shymkent 160012, Kazakhstan; syaljo@mail.ru (A.S.); narmanov70@bk.ru (M.N.)
[4] Department of Chemistry, L. Gumilyev Eurasian National University, Astana 010000, Kazakhstan; articova@mail.ru
[5] Branch of the Gubkin Russian State University of Oil and Gas, Tashkent 100125, Uzbekistan; sidikov_a@mail.ru
* Correspondence: guzalita.f1978@mail.ru (G.S.); 17tile@gmail.com (A.T.)

Abstract

This study evaluates natural zeolite from the Chankanay deposit modified with cobalt (ZMC) and nickel (ZMN) ions as an alternative to conventional metal naphthenate adhesion promoters in isoprene rubber compounds bonded to brass-plated steel cord. The modified zeolites were characterized by scanning electron microscopy (SEM), energy-dispersive X-ray spectroscopy (EDS) with elemental mapping, X-ray photoelectron spectroscopy (XPS), and Fourier-transform infrared spectroscopy (FTIR). EDS indicated cobalt and nickel contents of 2.6 and 1.0 wt.%, respectively. At the optimal loading of 9.12 phr, which completely replaced the naphthenate, the maximum rheometric torque was 33.0 N·m, equal to that of the reference compounds. Tensile strength reached 20.39 MPa (ZMC) and 20.33 MPa (ZMN), tear resistance 84.3 and 82.6 kN/m, and bond strength 305 and 310 N, respectively. At 100 °C, the bond strength was 18.0% (ZMC) and 14.9% (ZMN) higher than that of the corresponding reference compounds. The results indicate that Co- and Ni-modified natural zeolites are a promising alternative to naphthenate adhesion promoters, providing comparable mechanical properties and improved adhesion at elevated temperatures. Because compounds with unmodified zeolite were not prepared, the contributions of the zeolite framework and of the metals cannot be separated; the interfacial mechanisms and environmental aspects require further study.

Keywords: ion exchange; transition-metal immobilization; rubber-steel cord adhesion; brass-plated steel cord; vulcanization kinetics; zeolite-supported adhesion

Check for updates

Academic Editor: Claudia Belviso

Received: 30 October 2026
Revised: 21 November 2026
Accepted: 24 November 2026
Published: 27 November 2026

Copyright: © 2026 by the authors. Licensee MDPI, Basel, Switzerland. This article is an open access article distributed under the terms and conditions of the Creative Commons Attribution (CC BY) license.

1. Introduction

Elastomer–metal composites are widely used in the tire and rubber industries, particularly in products subjected to high mechanical stresses, repeated deformation, and dynamic loading. Metallic reinforcing elements, including wires, cables, and steel cords, improve the strength, stiffness, and dimensional stability of elastomeric products. However, differences in the mechanical and thermal properties of rubber and metal can promote stress concentration at their interface, making interfacial adhesion a critical factor determining the durability and service life of reinforced rubber products [1–3].

Improving the adhesion between rubber and metallic reinforcement is of considerable industrial importance because the reliability of rubber–metal composites depends on the integrity of the interfacial bond under mechanical, thermal, and environmental exposure. One widely used industrial approach is the direct bonding of rubber to brass-plated steel cord during vulcanization. This process involves interactions between sulfur-containing components of the rubber compound and the brass surface, leading to the formation of an interfacial layer containing copper sulfides. The composition, thickness, morphology, and stability of this layer influence the initial adhesion strength and its retention during service [4–8]. Consequently, developing effective adhesion-promoting systems is important for improving the performance and durability of rubber products used, for example, in tires, conveyor belts, and hoses.

Conventional adhesion-promoting systems commonly contain organic salts of transition metals, particularly cobalt stearate and cobalt naphthenate. These compounds influence interfacial reactions during vulcanization and can contribute to the formation and stability of the rubber–brass bond. However, excessive amounts of cobalt-containing additives may adversely affect the oxidative stability and processing characteristics of rubber compounds. In addition, concerns regarding cobalt consumption, material costs, and potential environmental and health impacts have stimulated interest in alternative adhesion-promoting systems that use transition metals more efficiently [9–14]. The principal challenge is therefore to reduce the dependence on conventional metal-based promoters without compromising the mechanical properties of rubber compounds or their adhesion to brass-plated steel cord. Reducing the use of cobalt-containing additives is also relevant from the resource and environmental points of view.

One potential approach involves the incorporation of transition-metal-containing species into porous mineral carriers. Natural zeolites are aluminosilicate materials characterized by ion-exchange properties, thermal stability, and the ability to accommodate various metal cations [15,16]. Kazakhstan possesses significant reserves of natural zeolite, including the Chankanay deposit, which makes it an accessible and low-cost carrier. The use of such carriers may provide an alternative means of introducing metal-containing components into rubber formulations. In particular, modification of natural zeolite with cobalt or nickel ions offers a possible route to developing mineral-supported adhesion promoters. However, the influence of such modified zeolites on rubber vulcanization, mechanical behavior, and rubber–steel cord adhesion requires systematic experimental evaluation.

Previous studies have investigated different approaches to improving rubber–metal adhesion, including the use of conventional transition-metal salts, reduced-cobalt adhesion-promoting systems, and modified inorganic fillers [4,6–10,12]. The role of cobalt-containing species in rubber–brass interfacial interactions has also been examined [12]. In parallel, natural zeolites have attracted attention as functional additives in polymer materials [13,14]. Chen et al. [13] investigated organic-amine-modified natural zeolite as a filler in natural rubber, and Orazymbetova et al. [14] reviewed the applications of zeolites in different fields, highlighting their adsorption, ion-exchange, and functional properties. Our previous studies characterized the physicochemical properties of zeolites from the Chankanay deposit [15,16]; a utility model patent was obtained for a method of producing an adhesion promoter for bonding rubbers to metals [17]; and natural zeolite-based rubber compounds were developed for water-sealing applications [18]. These studies provide a basis for considering modified zeolites as potential components of rubber formulations.

Despite these developments, the use of natural zeolite separately modified with cobalt and nickel ions as an alternative to conventional metal naphthenate adhesion promoters in rubber compounds remains insufficiently investigated. In particular, comparative information is limited regarding the effects of cobalt- and nickel-modified zeolites on vulcanization

characteristics, mechanical properties, and adhesion to brass-plated steel cord under different testing conditions. Furthermore, the relationship between the elemental composition of modified zeolites and their adhesion-promoting performance has not been adequately established. These limitations identify the need for a systematic comparative investigation.

To address this research gap, the present study investigates natural zeolite from the Chankanay deposit in Kazakhstan [16,17], separately modified with cobalt and nickel ions, as a functional component of adhesion-promoting systems for isoprene rubber compounds. The proposed approach involves introducing metal-containing species through a zeolite carrier rather than using conventional metal naphthenates. The study evaluates whether these modified zeolites can provide mechanical and adhesion properties comparable to those of conventional adhesion promoters. The possible contribution of the zeolite carrier and metal-containing species to interfacial interactions is considered as a working hypothesis requiring further experimental verification.

The objective of this work is to characterize cobalt-modified zeolite (ZMC) and nickel-modified zeolite (ZMN) and to evaluate their effects on the processing, mechanical, and adhesion properties of rubber compounds reinforced with brass-plated steel cord. The modified zeolites are characterized using scanning electron microscopy (SEM), energy-dispersive X-ray spectroscopy (EDS), elemental mapping, X-ray photoelectron spectroscopy (XPS), and Fourier-transform infrared spectroscopy (FTIR). The effects of ZMC and ZMN on vulcanization behavior, tensile properties, tear resistance, and rubber–steel cord adhesion, including adhesion at an elevated temperature (100 °C), are examined and compared with those of reference compounds containing conventional metal naphthenate promoters. Finally, hypothetical mechanisms of the influence of ZMC and ZMN on the rubber–brass adhesive interface are proposed to support the interpretation of the experimental findings. The environmental implications of the proposed approach are identified as an area requiring further investigation.

2. Materials and Methods

The following materials were studied: natural zeolite from the Chankanay deposit, modified with cobalt ions (ZMC) and nickel ions (ZMN).

The zeolite-bearing rock samples were collected from the Chankanay deposit, located in the Kerbulak District of Almaty Region, Kazakhstan. The approved reserves of the deposit amount to 4.3 million tonnes [14]. The main mineralogical phase of the zeolite is heulandite-clinoptilolite, while quartz is the principal mineral impurity in the rock. Minor amounts of calcium- and iron-bearing compounds are also present in the form of micrometer-sized crystalline or amorphous phases. The initial elemental composition of the natural zeolite was determined by elemental analysis and was as follows: C—4.89%, O—50.84%, Si—21.92%, Al—7.41%, Ca—3.98%, Na—1.56%, K—1.61%, Mg—1.95%, and Fe—5.84% [15].

The natural zeolite samples were initially prepared by primary crushing of the raw rock in a standard crusher, followed by sieving to obtain a particle size fraction of 1.0–1.4 mm. The selected fraction was washed with distilled water to remove clay impurities and dried at 95–100 °C. Prior to incorporation into the rubber compounds, the zeolite was additionally finely ground in a laboratory ball mill at 100 rpm for 120 min, followed by control sieving through a 63 μm sieve. Therefore, the 1.0–1.4 mm fraction refers to an intermediate stage of zeolite preparation and does not represent the final particle size of the filler introduced into the rubber matrix. The particle size distribution (D50) of the ground powder was not determined; the powder used for mixing passed through a 63 μm sieve.

Modification of natural zeolite can be achieved through single-stage or multi-stage processes, including thermal activation and chemical treatment using acids, alkalis, or

inorganic salts [19]. In this work, acid treatment, thermal treatment, and ion exchange were applied. Acid treatment is known to cause dealumination, i.e., a decrease in the aluminum content of the zeolite, and to increase its pore volume [19,20].

Acid treatment. Acid treatment was carried out by treating 10 g of pretreated zeolitic tuff (sieved, washed, and dried) with 100 mL of 1.0 mol/L hydrochloric acid (HCl) solution in a shaking water bath (OLS26 Aqua Pro, Grant Instruments, Beaver Falls, PA, USA) operating in linear mode at 75 °C for 1 h. After acid treatment, the sample was washed with distilled water at room temperature until Cl^- ions were no longer detected in the washing water, as verified using an $AgNO_3$ solution. The sample was then dried and weighed to determine the mass loss. The mass loss after acid treatment was 7.4%.

Thermal treatment. The prepared samples were placed in heat-resistant round-bottomed crucibles and thermally treated in a B400/410 muffle furnace (Nabertherm, Lilienthal, Germany) at 100 °C under static conditions for 1 h. After the thermal treatment, the crucibles containing the zeolite samples were placed in desiccators with calcined $CaCl_2$ and allowed to cool completely.

Ion exchange with Ni^{2+} and Co^{2+}. Ion exchange for the preparation of nickel- and cobalt-containing zeolites was carried out in a combined orbital-linear shaking water bath (OLS26 AquaPro, Grant Instruments) using 0.5 mol/L aqueous solutions of $NiCl_2$ and $CoCl_2$ (1 equiv/L with respect to the divalent metal cations). The solid-to-solution ratio was 1:6 (w/v; 10 g of zeolite per 60 mL of solution). Three consecutive treatments of 1 h each were carried out, each with a fresh portion of the solution. To intensify the ion exchange, the water bath was maintained at 80–90 °C with continuous shaking (150 rpm). After each treatment, the zeolite was washed with distilled water using a filter-paper-lined funnel until chloride ions (Cl^-) were no longer detected in the filtrate. The washed zeolite was subsequently air-dried and then dried in an oven at 90–95 °C [16,17].

Characterization. Microscopic studies were performed using a research complex based on a Supra SSVP field-emission electron microscope (SEM, Figure 1). The elemental composition of the samples (Tables 1 and 2) was determined by energy-dispersive X-ray spectroscopy (EDS; EDS spectra and elemental mapping are shown in Figures 2–5).

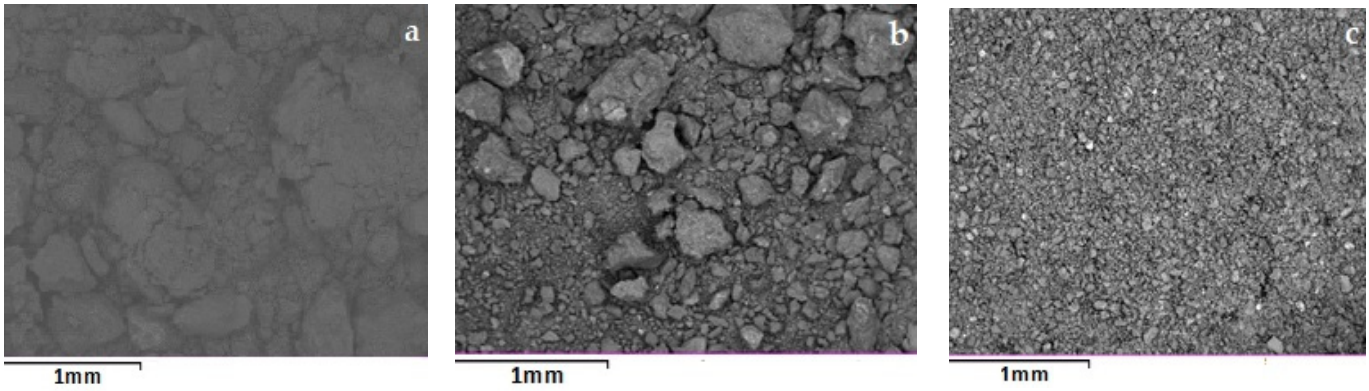


Figure 1. SEM micrographs of zeolite samples: natural zeolite (**a**), ZMC (**b**), and ZMN (**c**). Scale bar: 1 mm.

Table 1. Elemental compositions of the studied ZMC.

Element	O	Mg	Al	Si	K	Ca	Fe	Co
Wt. %	48.8	2.1	8.2	23.4	2.1	4.3	8.5	2.6

Table 2. Elemental compositions of the studied ZMN.

Element	O	Mg	Al	Si	K	Ca	Ti	Fe	Ni
Wt. %	53.7	1.5	8.7	24.5	1.8	1.8	0.5	6.5	1.0

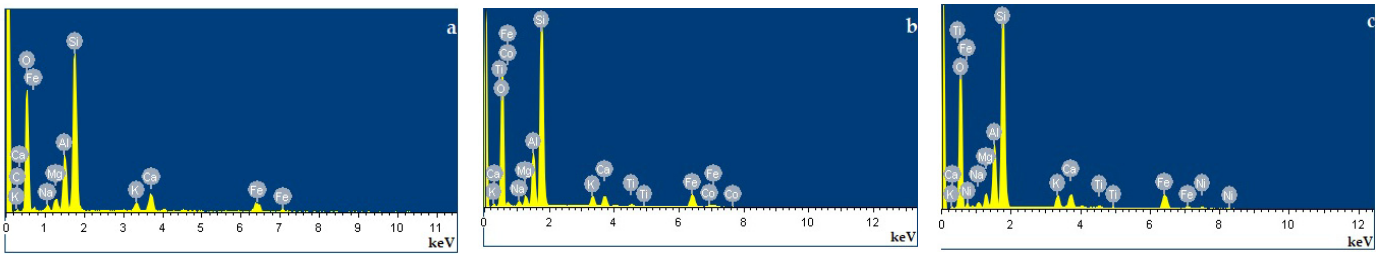


Figure 2. EDS spectra of the zeolite samples: (**a**) natural zeolite, (**b**) ZMC, (**c**) ZMN.

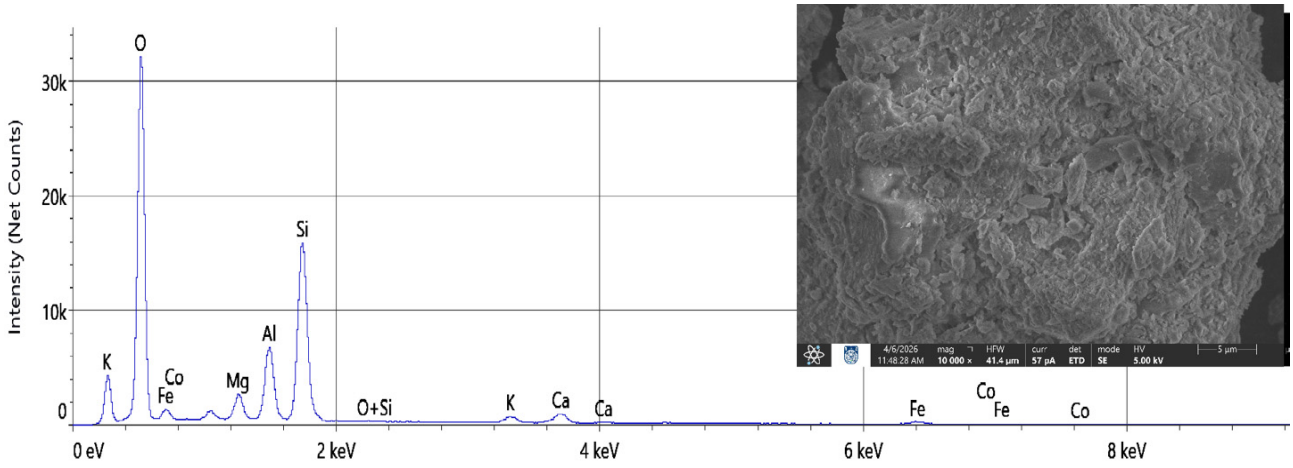


Figure 3. EDS analysis showing the elemental composition and scanned image of the ZMC.

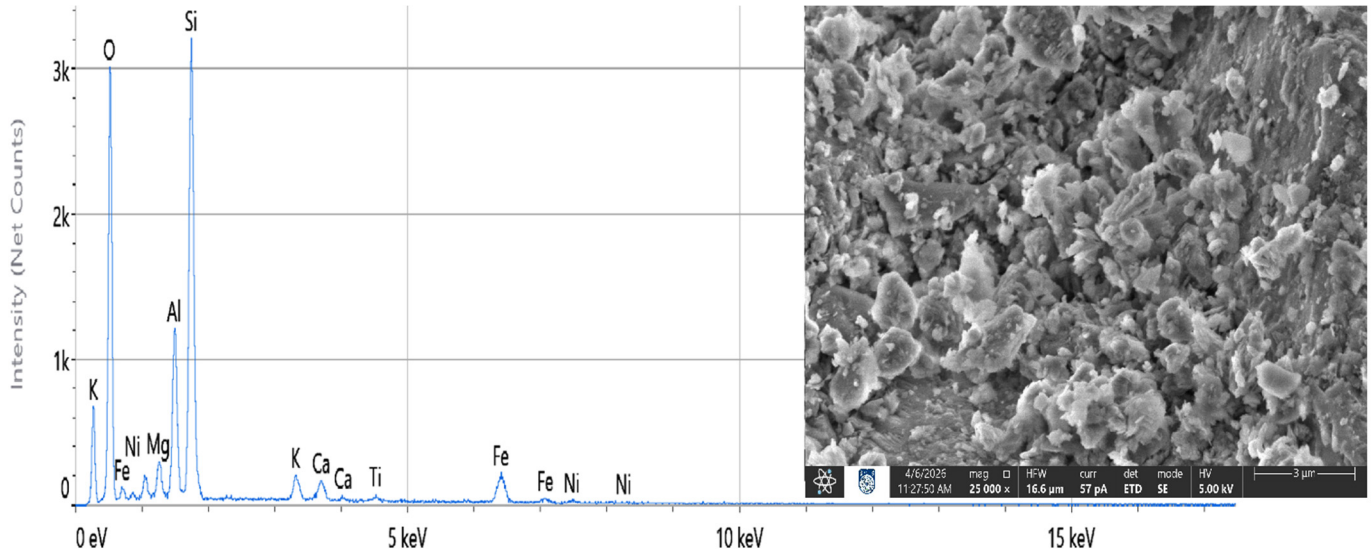


Figure 4. EDS analysis showing the elemental composition and scanned image of the ZMN.

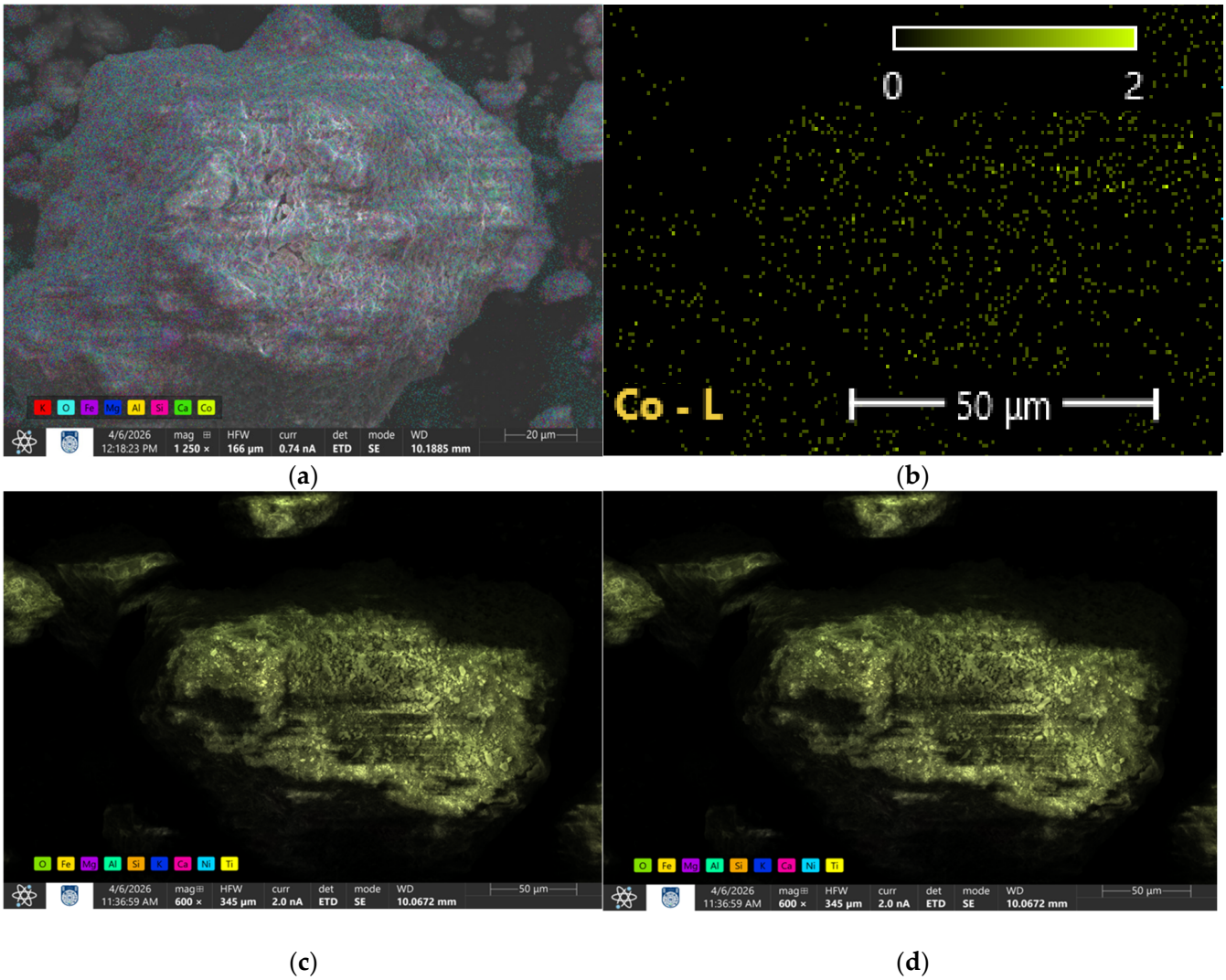


Figure 5. Distribution map of Co (II) and Ni (II) in the zeolite: (**a**) EDS mapping of the cobalt-modified zeolite, (**b**) EDS mapping of Co (II) distribution; (**c**) EDS mapping of the nickel-modified zeolite; (**d**) EDS mapping of Ni (II) distribution.

Surface analysis of the samples was performed using X-ray photoelectron spectroscopy (XPS). The Co 2p and Ni 2p regions of ZMC and ZMN were recorded on a Thermo Fisher Scientific Nexsa XPS spectrometer (Waltham, MA, USA) using monochromated Al Kα radiation (1486.6 eV, 72 W). The binding energy scale was verified using a sputter-cleaned Ag reference. High-resolution spectra were acquired at a pass energy of 50 eV, and the measurements were performed using Avantage software (v6.8.1). The spectra are shown in Figure 6 without background subtraction or peak fitting.

FTIR spectra of the ZMC and ZMN samples were recorded using a Shimadzu IR Prestige-21 FTIR spectrometer equipped with a Miracle attenuated total reflectance (ATR) accessory (Pike Technologies, Fitchburg, WI, USA). The samples were analyzed in ATR mode, allowing direct spectral measurement without preparation of KBr pellets. The spectra were recorded over the range of 4000–400 cm^{-1} at a spectral resolution of 4 cm^{-1} using 32 accumulated scans. Baseline correction was applied.

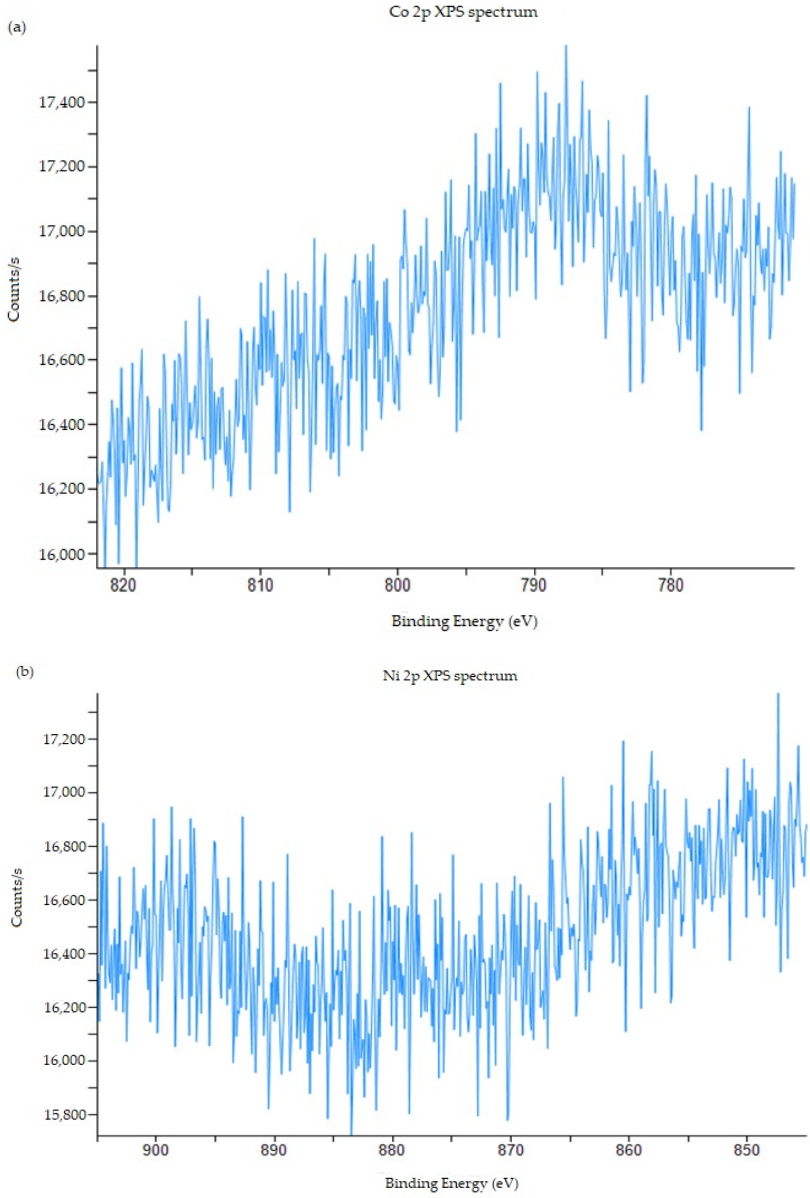


Figure 6. XPS analysis: ZMC (**a**) and ZMN (**b**) spectra. Spectra are shown without background subtraction or peak fitting.

2.1. Preparation of Rubber Compounds

Rubber compounds containing cobalt- and nickel-modified zeolites (ZMC and ZMN) were prepared according to the general compounding procedure reported previously [21]. The modified zeolites were incorporated into an SKI-3 isoprene rubber matrix (initial plasticity 0.30–0.40) at loadings of 6.0–10.0 parts per hundred parts of rubber (phr). In formulations 1–4, the cobalt or nickel naphthenate content was progressively reduced and replaced with ZMC or ZMN, while the total promoter content (naphthenate plus modified zeolite) was maintained at 9.12 phr; in formulation 5, ZMC or ZMN was used at 10.0 phr without naphthenate (Tables 3 and 4). As described above, the modified zeolites were ground and passed through a 63 μm sieve before being incorporated into the rubber compounds.

Table 3. Breaker rubber compound containing ZMC zeolite.

№	Material Name	Weight Parts 100 Pts. Wt Rubber					
		Standard	**1**	**2**	**3**	**4**	**5**
1	SKI-3	100.0	100.0	100.0	100.0	100.0	100.0
2	Technical sulfur	1.6	1.6	1.6	1.6	1.6	1.6
3	Polymer sulfur	1.89	1.89	1.89	1.89	1.89	1.89
4	Sulfenamide C	1.2	1.2	1.2	1.2	1.2	1.2
5	Santogard PV	0.29	0.29	0.29	0.29	0.29	0.29
6	Modifier RU	0.98	0.98	0.98	0.98	0.98	0.98
7	Hepsol COD	0.40	0.40	0.40	0.40	0.40	0.40
8	Zinc white	6.47	6.47	6.47	6.47	6.47	6.47
9	Stearic acid	0.91	0.91	0.91	0.91	0.91	0.91
10	Pine rosin	1.89	1.89	1.89	1.89	1.89	1.89
11	Oil of PN-6Sh	5.09	5.09	5.09	5.09	5.09	5.09
12	Acetonanil P	0.41	0.41	0.41	0.41	0.41	0.41
13	Diaphene AF	0.98	0.98	0.98	0.98	0.98	0.98
14	Cobalt naphthenate	9.12	3.12	2.12	1.12	-	-
15	ZMC	-	6.0	7.0	8.0	9.12	10.0
16	Structol	0.09	0.09	0.09	0.09	0.09	0.09
17	TU P—234	51.09	51.09	51.09	51.09	51.09	51.09
	Total:	182.41	182.41	182.41	182.41	182.41	183.29

The reference compounds (denoted "Standard" in the tables and figures) contained cobalt naphthenate (reference for the ZMC series) or nickel naphthenate (reference for the ZMN series) at 9.12 parts by weight per 100.0 parts by weight of rubber.

Rubber compounds were prepared in two stages using a laboratory two-roll mill (LB 320-160/160) at a roll surface temperature of 60 ± 5 °C. The rotational speeds of the front and rear rolls were (29 ± 1) and (36 ± 1) rpm, respectively, corresponding to a friction ratio of 1:1.25.

During the first mixing stage, the entire amount of rubber was loaded onto the mill and masticated for 3 min, and mixing was then continued until 8 min. The powdered ingredients, including the modified zeolite, and one-half of the total carbon black were subsequently introduced during the 8–12 min interval. The plasticizers (oil components) and the remaining half of the carbon black were added during the 12–17 min interval, and mixing was continued until 18 min. The compound was removed from the mill between 18 and 20 min. All ingredients except the accelerator and sulfur were incorporated during this stage. The total duration of the first mixing stage was 20 min. The resulting compound was allowed to rest for at least 2 h before the second mixing stage.

During the second stage, the first-stage compound was loaded onto the mill and heated for 2 min. The accelerator and sulfur were then added, and mixing was carried out during the 2–5 min interval. The finished compound was removed from the mill between 5 and 6 min. The total duration of the second mixing stage was 6 min, and the total mixing time for both stages was 26 min (20 + 6 min).

Table 4. Breaker rubber compound containing ZMN.

№	Material Name	Weight Parts 100 Pts.Wt Rubber					
		Standard	1	2	3	4	5
1	SKI-3	100.0	100.0	100.0	100.0	100.0	100.0
2	Technical sulfur	1.6	1.6	1.6	1.6	1.6	1.6
3	Polymer sulfur	1.89	1.89	1.89	1.89	1.89	1.89
4	Sulfenamide C	1.2	1.2	1.2	1.2	1.2	1.2
5	Santogard PV	0.29	0.29	0.29	0.29	0.29	0.29
6	Modifier RU	0.98	0.98	0.98	0.98	0.98	0.98
7	Hepsol COD	0.40	0.40	0.40	0.40	0.40	0.40
8	Zinc white	6.47	6.47	6.47	6.47	6.47	6.47
9	Stearic acid	0.91	0.91	0.91	0.91	0.91	0.91
10	Pine rosin	1.89	1.89	1.89	1.89	1.89	1.89
11	Oil of PN-6Sh	5.09	5.09	5.09	5.09	5.09	5.09
12	Acetonanil P	0.41	0.41	0.41	0.41	0.41	0.41
13	Diaphene AF	0.98	0.98	0.98	0.98	0.98	0.98
14	Nickel naphthenate	9.12	3.12	2.12	1.12	-	-
15	ZMN	-	6.0	7.0	8.0	9.12	10.0
16	Structol	0.09	0.09	0.09	0.09	0.09	0.09
17	TU P—234	51.09	51.09	51.09	51.09	51.09	51.09
	Total:	182.41	182.41	182.41	182.41	182.41	183.29

The prepared rubber compounds were vulcanized in a hydraulic press at 155 °C for 15 min.

2.2. Testing of Rubber Compounds

The plastic-elastic, technological, physical-mechanical, and adhesion properties of the rubber compounds were evaluated. For each series (ZMC and ZMN), the reference compound and five experimental compounds were prepared. Based on the results of repeated measurements, the mean values (M), standard deviation (SD), coefficient of variation (CV = SD/M × 100%), and relative half-width of the 95% confidence interval (Δ95) were calculated. The statistical significance of differences between the compounds within each series was assessed using one-way analysis of variance (ANOVA, p).

The plasticity of the rubber compounds was determined in accordance with GOST 415-75 [22] using a Williams compression plastometer (Yasuda Seiki Seisakusho, Ltd., Nishinomiya, Japan); ASTM D926 was used as the corresponding international equivalent. Vulcanization characteristics were determined in accordance with GOST 12535-84 [23] using an MDR-2000 rotorless vulcameter (equivalent to ASTM D5289) (Alpha Technologies (formerly Monsanto), Akron, OH, USA). The tensile properties of the vulcanizates were determined in accordance with GOST R 54553 [24] (equivalent to ASTM D412) using an RMI-60 tensile testing machine (ZIM Tochmashpribor, Armavir, Russia). Tear resistance and Shore A hardness were determined in accordance with GOST 262-93 [25] and GOST 263-75 [26], respectively. The bond strength between rubber and brass-plated steel cord was determined by the pull-out test in accordance with GOST ISO 5603-2013 [27] (analog of ASTM D2229) under the following conditions: at 20 °C; at 100 °C; after thermal aging in air at 120 °C for 16 h; and after salt aging by boiling in a 5% NaCl solution for 6 h. The

cord embedment length was 10 mm, and the crosshead speed during the pull-out test was 50 mm/min. Six specimens were tested for each compound and condition.

3. Results and Discussion

As previously reported [16,17] the surface of the zeolite particles contains active centres, including radical ion-radical sites, oxide and hydroxide groups that are capable of interacting with multivalent metal cations, particularly Co^{2+} and Ni^{2+}, widely used as components of traditional rubber adhesion promoters to metal cord; the mechanism of action of these promoters is well known [4–6].

The composition of the zeolite, especially the Si/Al ratio, and the cationic form, strongly influences its adsorption properties [28–30]. As Si/Al ratio grows, the polarity of the zeolite is known to decrease [28,29]. According to previous data [16], the Chankanay zeolite is in Na^+ form and has a molar ratio of Si/Al = 3–3.6, which corresponds to the relatively high polarity [16].

The elemental composition and morphology of the natural and modified zeolites were studied by EDS and SEM (Figures 1–5).

Figure 1 presents SEM images of natural zeolite (a), cobalt-modified zeolite (ZMC, b), and nickel-modified zeolite (ZMN, c) obtained at low magnification (scale bar 1 mm). At this magnification, the images reflect the particle shape, size, and overall appearance of the samples rather than the surface morphology of individual crystals. The natural zeolite consists of relatively large, irregularly shaped particles and agglomerates. The ZMC sample shows a more fragmented structure, with angular particles of varying sizes and smaller fragments distributed between larger agglomerates. In contrast, the ZMN sample exhibits a visually finer and more uniform granular appearance, with fewer prominent large agglomerates than ZMC.

These observations indicate differences in the apparent particle size and shape of the investigated samples. However, these differences cannot be unambiguously attributed to the incorporation of Co^{2+} or Ni^{2+} ions, since grinding and sample preparation may also influence the particle morphology. The particle size distribution was not determined, and images at higher magnification would be required to evaluate the surface morphology.

The EDS spectra of natural zeolite, ZMC, and ZMN are shown in Figure 2. They confirm the presence of cobalt and nickel in the samples after treatment with $CoCl_2$ and $NiCl_2$ solutions; EDS does not identify the oxidation state of the metals or the way they are bound to the framework. Cobalt and nickel cations are expected to interact with the active sites of the zeolite, which may lead to their fixation on the zeolite particles and give them the properties of adhesion promoters to metal cord. A possible synergistic effect of the contact between Co^{2+} and Ni^{2+} cations and cations of other metals present in the zeolite has also been suggested [31].

Natural zeolites have ion-exchange properties due to a developed system of cavities and channels in the crystal lattice. These cavities contain water molecules and large mobile cations, mainly alkali and alkaline-earth metals (Na^+, K^+, Ca^{2+}, Mg^{2+}), which provide the ion-exchange capacity of the material. However, the contribution of calcium and magnesium cations to the adsorption process is reported to be small. A decrease in the pH of the test solution (from 5.5 to 5.0) indicates a possible adsorption mechanism involving the replacement of H^+ ions of the hydroxyl groups of the zeolite structure [32,33].

To visualize the distribution of Co^{2+} and Ni2+ ions in the modified zeolite, additional studies were conducted using EDS mapping. The energy-dispersive spectra of the studied samples are shown in Figures 3–5.

The EDS results for the modified zeolites are shown in Figure 3 (ZMC) and Figure 4 (ZMN). According to the EDS results, the samples contain O, Mg, Al, Si, K, Ca, and

Fe (and Ti in ZMN), together with the corresponding modifying metals. The elemental compositions of ZMC and ZMN are presented in Tables 1 and 2, respectively. The cobalt content in ZMC was 2.6 wt.%, whereas the nickel content in ZMN was 1.0 wt.%. These values are semi-quantitative and characterize the analyzed regions. In addition, EDS does not distinguish between metal species located on the external surfaces of the particles and those incorporated into the internal pore structure of the zeolite.

From the elemental distribution maps (Figure 5), the distribution of the elements appears uniform within the analyzed areas, with no pronounced segregation observed. These findings indicate the presence of cobalt and nickel in the zeolite samples; however, no definitive conclusions regarding the formation of active sites or the homogeneity of metal distribution can be drawn from the EDS data alone.

The cobalt content in ZMC is higher than the nickel content in ZMN, although both samples were prepared by the same ion-exchange procedure. This difference should be interpreted with caution. EDS is a semi-quantitative technique that probes only local areas of the surface, and the natural zeolite is compositionally heterogeneous (for example, the Fe content differs between the samples: 8.5 wt.% in ZMC and 6.5 wt.% in ZMN). In addition, the Fe Kβ and Co Kα lines partially overlap in EDS spectra, which may affect the accuracy of the cobalt determination in iron-containing samples. The difference may also reflect different affinities of Co^{2+} and Ni^{2+} cations for the exchange sites of the aluminosilicate framework. Bulk analysis (e.g., AAS or ICP) would be required to establish the metal uptake reliably.

Despite its lower nickel content, ZMN showed a bond strength slightly higher than that of ZMC (see the adhesion results below). This suggests that the total metal content determined by EDS does not by itself explain the differences in adhesion performance. The accessibility and distribution of the metal-containing species may also influence their effectiveness; however, these factors were not quantified in the present study, so the relationship between metal content, surface accessibility, and adhesion performance remains to be established.

X-ray photoelectron spectroscopy (XPS) provides information on the chemical composition and electronic states of elements in the near-surface layer of materials [34]. XPS has been applied to the surface analysis of natural and cation-exchanged zeolites [35–37] and of Ni-modified aluminosilicates [38]. The Co 2p and Ni 2p regions of ZMC and ZMN, respectively, are shown in Figure 6.

The spectra have a low signal-to-noise ratio, and no well-defined Co 2p or Ni 2p peaks or satellite structures can be reliably distinguished. Consequently, background subtraction (e.g., Shirley or Tougaard), peak deconvolution, and spin–orbit doublet analysis could not be performed, and the oxidation states of cobalt and nickel cannot be determined from these data. On the basis of the ion-exchange procedure ($CoCl_2$ and $NiCl_2$ solutions), the metals are expected to be present as Co^{2+} and Ni^{2+}, but this was not independently confirmed by XPS. The presence of cobalt and nickel in the samples is supported by EDS (Tables 1 and 2). Reliable determination of the chemical states requires high-resolution measurements with longer acquisition times, appropriate background subtraction, and quantitative peak fitting [34].

Infrared spectroscopy is a useful tool for studying the interaction between zeolite and sorbed ions. Therefore, the subsequent analysis focused on the sorption Co^{2+} and Ni^{2+} ions on the zeolite surface using FTIR spectroscopy. Previous studies [15,16] presented FTIR data for untreated and acid-treated Chankanay zeolite obtained using a Shimadzu IR Prestige-21 spectrometer equipped with a Miracle ATR accessory (Pike Technologies, Fitchburg, WI, USA).

Figure 7 presents the IR spectra of the natural zeolite from Chankanay zeolite modification with Ni^{2+} (1) and Co^{2+} (2) ions. The spectra show the stretching and bending vibrations

of the structural groups of the aluminosilicate framework. Following modification with Co^{2+} and Ni^{2+}, additional absorption band appears at approximately 914 cm^{-1}, which may be associated with vibrations involving metal-oxygen bonds. In the regions of stretching and bending vibrations of the framework, the Ni^{2+}-modified zeolite shows an additional band at approximately 475–500 cm^{-1}, whereas Co^{2+} modification is accompanied by a broadened absorption band at approximately 515–540 cm^{-1} [39,40].

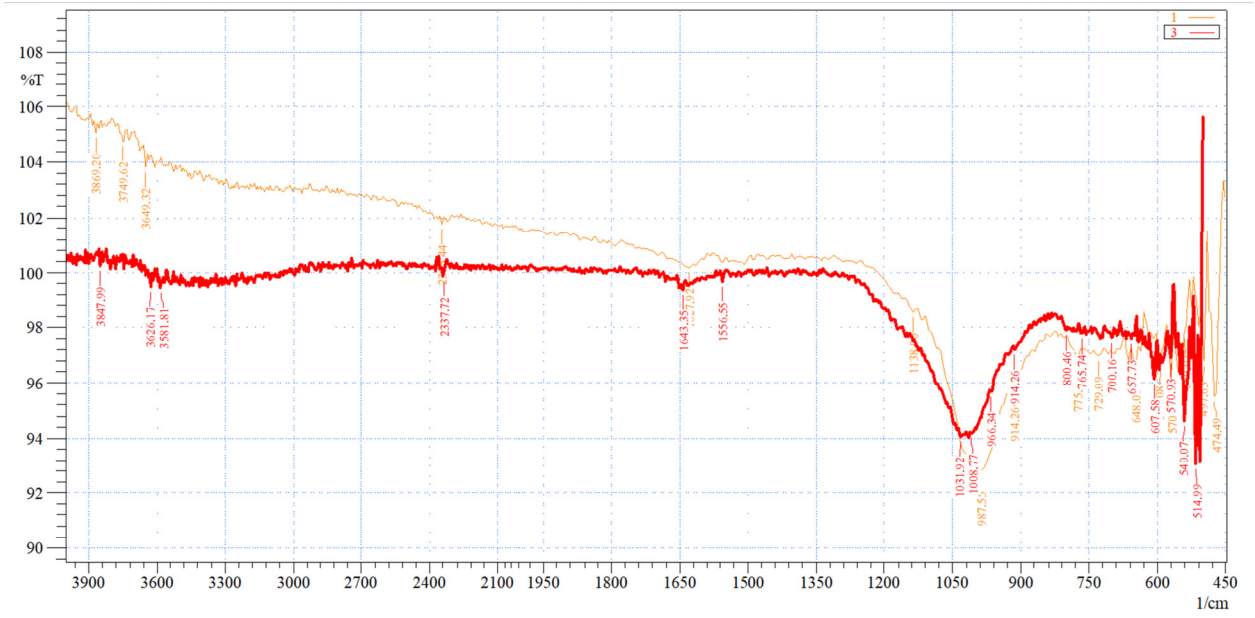


Figure 7. IR spectra of ZMN (1) and ZMC (2).

Previous studies [41] have shown that donor–acceptor interactions constitute an important mechanism of metal-ion adsorption on aluminosilicates, as indicated by characteristic changes in the regions corresponding to Si-O stretching and O-Si-O bending vibrations. Ion exchange involving the Ca^{2+} and Mg^{2+} cations of the zeolite framework occurs to a limited extent and is not considered the dominant mechanism under the studied conditions. Adsorption involving hydroxyl groups accounts for no more than 5–10% of the total adsorption capacity [41]. Therefore, the changes observed in the IR spectra of the modified zeolites, particularly in the 600–400 cm^{-1} region, indicate interactions between Ni^{2+} and Co^{2+} ions and the zeolite structure; however, FTIR alone does not allow the contributions of ion exchange and other adsorption mechanisms to be distinguished.

To evaluate the possibility of using the Chankanay zeolite modified with Co^{2+} and Ni^{2+} as a promoter of rubber adhesion to steel cord, the effects of the modified zeolites and of their dosage on the kinetics of sulfur vulcanization and on the physical and mechanical properties of the vulcanizates were studied.

The experimental formulations were designed according to a stepwise substitution approach rather than on the basis of equivalent metal content. The dosage of ZMC or ZMN was increased stepwise (6.0, 7.0, 8.0, 9.12, and 10.0 phr in formulations 1–5), while the content of cobalt or nickel naphthenate was correspondingly reduced (3.12, 2.12, and 1.12 phr in formulations 1–3; no naphthenate in formulations 4 and 5), which allowed the effectiveness of partial and complete replacement of the conventional promoter to be evaluated. In formulations 1–4, the total promoter content (naphthenate plus modified zeolite) was kept at 9.12 phr, as in the reference compound, whereas formulation 5 contained 10.0 phr of ZMC or ZMN (Tables 3 and 4). The optimum formulation was obtained under complete replacement of the naphthenate with ZMC or ZMN (formulation 4). Because

compounds containing unmodified zeolite at the same loadings were not prepared, the effects of the mineral filler and of the incorporated metal species cannot be distinguished.

No processing difficulties were observed during the preparation of the compounds.

Rheometric cure curves are used to evaluate the processing and vulcanization characteristics of rubber compounds, providing information on the duration of the vulcanization induction period, the time required to reach the optimum cure, and the vulcanization plateau [42]. The characteristics of the vulcanization plateau depend on the curing temperature, which can affect the mechanical properties of the resulting vulcanizate [43]. The width and stability of the plateau are related to the rate of reversion. Reversion behavior is strongly influenced by the curing temperature and the type and structure of crosslinks formed by the vulcanization system [43,44].

The plasticity of the compounds is shown in Figure 8 and Tables 5 and 6. For the compounds containing ZMC and ZMN, it ranged from 0.28 to 0.31, i.e., within the specified range of 0.30 ± 0.05, and the compounds are classified as having medium plasticity. A slight decrease was observed at the highest dosage (0.28 at 10.0 phr), which may be related to the higher content of the mineral component; no clear trend was found for ZMN.

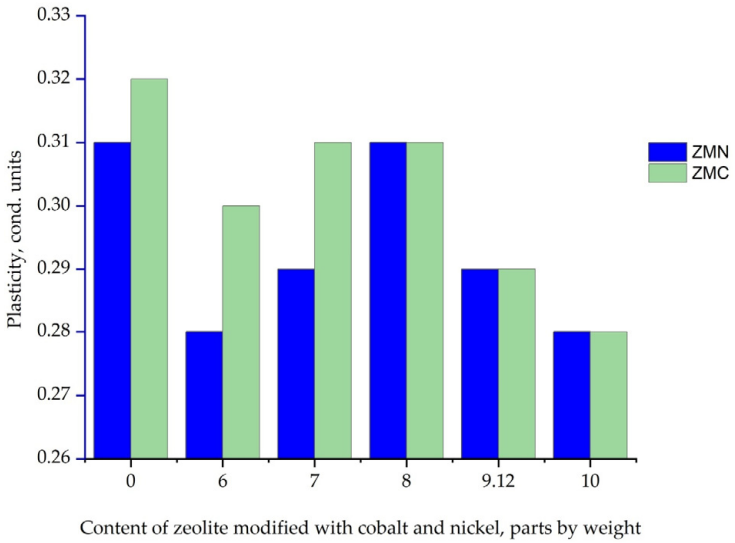


Figure 8. Plasticity of the breaker rubber compounds containing ZMC and ZMN.

Table 5. Plastic-elastic properties of rubber compounds containing ZMC.

Name of Indicators	Sample Numbers					
	Standard	**1**	**2**	**3**	**4**	**5**
Plasticity, cond. units 0.30 ± 0.05	0.32	0.30	0.31	0.31	0.29	0.28
Minimum torque, N·m	8.0	9.0	9.5	8.5	9.5	10.0
Vulcanization start time, min	1 min 30 s	1 min 50 s	1 min 50 s	1 min 35 s	1 min 40 s	1 min 30 s
Moment in optimum of M_3 vulcanization, N·m	30.5	31.5	31.1	30.55	30.65	28.0
Time to achieve optimum vulcanization t_3, min	13 min 25 s	13 min 30 s	13 min 35 s	13 min 30 s	13 min 20 s	13 min 15 s
Maximum M_4 torque, N·m	33.0	34.0	33.5	33.0	33.0	30.0
Time to reach maximum degree of vulcanization, t_4, min	15 min	14 min	15 min	15 min	15 min	17 min

Table 6. Plastic-elastic properties of rubber compounds containing ZMN.

Name of Indicators	Sample Numbers					
	Standard	**1**	**2**	**3**	**4**	**5**
Plasticity, cond. units 0.30 ± 0.05	0.31	0.28	0.29	0.31	0.29	0.28
Minimum torque, N·m	9.0	9.5	10.5	9.2	10.0	11.0
Vulcanization start time, min	1 min 45 s	1 min 55 s	1 min 55 s	1 min 45 s	1 min 40 s	1 min 40 s
Moment in optimum of M_3 vulcanization, N·m	30.6	31.55	30.75	29.72	30.7	28.55
Time to achieve optimum vulcanization t_3, min	13 min 35 s	13 min 40 s	13 min 45 s	13 min 40 s	13 min 25 s	13 min 25 s
Maximum M_4 torque, N·m	33.0	34.0	33.0	32.0	33.0	30.5
Time to reach maximum degree of vulcanization, t_4, min	15 min	14 min	15 min	15 min	15 min	16 min

The vulcanization kinetics of the compounds were assessed from rheometric curves recorded on an MDR 2000 moving die rheometer (Alpha Technologies, Hudson, OH, USA) (Tables 5 and 6, Figures 9 and 10).

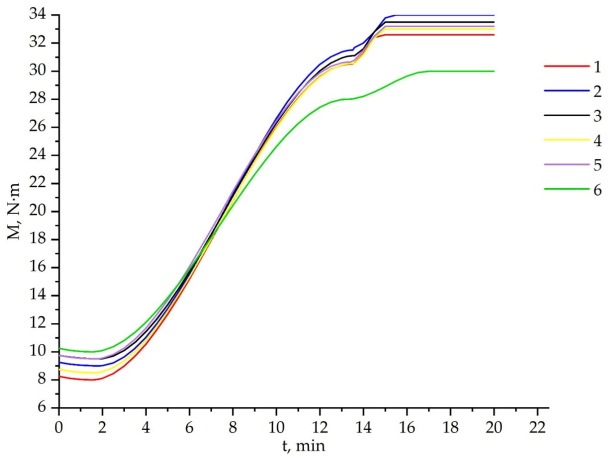


Figure 9. Vulcanization kinetics curves of SKI-3-based rubber compounds containing ZMC: 1—standard (reference compound); 2–6—formulations 1–5 (ZMC content 6.0, 7.0, 8.0, 9.12, and 10.0 phr). The compositions of the formulations are given in Table 3, and the rheometric characteristics derived from the curves are given in Table 5.

The rheometric curve is a graphical representation of the structuring of the elastomer composite.

A comparison of the data in Tables 5 and 6 shows that ZMC and ZMN have a similar effect on the vulcanization kinetics of the rubber compounds. The minimum torque increased compared with the reference (from 8.0–9.0 N·m to 8.5–11.0 N·m), which suggests an increase in the viscosity of the compounds that may be related to the introduction of the mineral component. The vulcanization onset time changed only slightly (1 min 30 s–1 min 55 s, versus 1 min 30 s and 1 min 45 s for the references). The time to reach optimum vulcanization (t_3) varied within 13 min 15 s–13 min 45 s, i.e., the technological stability of the process was maintained. The torque at the optimum ($M_3 \approx$ 28.0–31.6 N·m) was generally comparable to that of the references. The maximum torque (M_4) of formulations 1–4 (32.0–34.0 N·m) was comparable to the reference value (33.0 N·m). For formulation 5, M_3 and M_4 decreased (to 28.0–28.55 and 30.0–30.5 N·m, respectively), which may be related to an excess of modified zeolite (for example, adsorption of vulcanization ingredients on the zeolite surface or shielding of active sites); this was not verified in the present study.

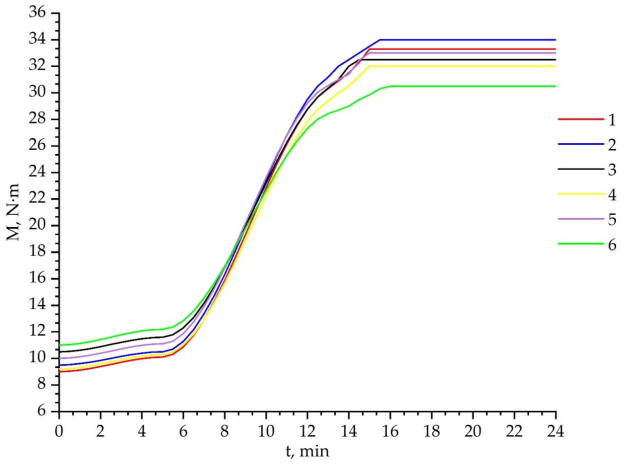


Figure 10. Vulcanization kinetics curves of SKI-3-based rubber compounds containing ZMN: 1—standard (reference compound); 2–6—formulations 1–5 (ZMN content 6.0, 7.0, 8.0, 9.12, and 10.0 phr). The compositions of the formulations are given in Table 4, and the rheometric characteristics derived from the curves are given in Table 6.

Thus, ZMC and ZMN have a similar effect on the vulcanization characteristics: they increase the minimum torque, change the onset time only slightly, and, at 6.0–9.12 phr, give maximum torque values comparable to the reference; at 10.0 phr the torque decreases. Without compounds containing unmodified zeolite, these effects cannot be assigned separately to the zeolite framework and to the metal ions.

Of particular interest is the comparison of the rheometric characteristics of compounds in which the conventional naphthenate-based promoters were completely replaced with modified zeolites. At a ZMC or ZMN loading of 9.12 phr, the maximum torque (M_4) reaches 33.0 N·m for both systems, corresponding to the values obtained for the respective reference compounds. This indicates that a comparable resistance to deformation during vulcanization can be maintained after complete replacement of the conventional adhesion promoters.

A further increase in the modified zeolite content to 10.0 phr results in a decrease in the maximum torque to 30.0 N·m for ZMC and 30.5 N·m for ZMN, corresponding to reductions of approximately 9.1% and 7.6%, respectively, relative to the reference values. This concentration-dependent behavior indicates that increasing the modified zeolite content beyond a certain level does not provide additional improvements in the rheometric characteristics of the compounds. Possible explanations include changes in filler dispersion, reduced availability of vulcanization ingredients due to their adsorption on the zeolite surface, and changes in interactions between the polymer matrix and modifier particles. However, these interpretations require further experimental verification. It should also be emphasized that rheometric torque reflects the combined mechanical response of the compound and cannot be considered a direct quantitative measurement of chemical crosslink density.

The use of ZMC and ZMN influences the sulfur vulcanization of rubber compounds, as shown by the change in the time to reach the maximum degree of vulcanization (t_4), which varied from 14 to 17 min for ZMC and from 14 to 16 min for ZMN. The maximum torque depends on the promoter dosage. At the optimal dosage of 9.12 phr, it is 33.0 N·m for both ZMC and ZMN compounds, equal to the reference value (33.0 N·m); at 10.0 phr, it decreases to 30.0 and 30.5 N·m, respectively (Figures 9 and 10). These results suggest that ZMC and ZMN can be used as adhesion promoters in rubber compounds.

The results of the physical, mechanical and adhesion tests of the obtained vulcanizates are shown in Tables 7 and 8 and Figure 11. The individual results of six replicate measurements for each formulation are provided in Supplementary Table S1 (ZMC) and Supplementary Table S2 (ZMN).

Table 7. Physicomechanical properties of vulcanizates containing ZMC and statistical evaluation of test results.

Name of Indicators	Standard	Weight Parts 100 Pts.Wt Rubber					ANOVA, *p*
		1	2	3	4	5	
Conventional tension at 300% elongation, MPa	14.71 ± 0.058	14.25 ± 0.051	14.45 ± 0.053	14.55 ± 0.053	14.78 ± 0.058	14.45 ± 0.053	<0.001
CV, %	0.39	0.36	0.36	0.36	0.39	0.36	
Δ95, %	0.41	0.38	0.38	0.38	0.41	0.38	
Conventional tensile strength, MPa	20.32 ± 0.058	19.80 ± 0.058	20.10 ± 0.058	20.28 ± 0.058	20.39 ± 0.058	20.21 ± 0.053	<0.001
CV, %	0.29	0.29	0.29	0.29	0.28	0.26	
Δ95, %	0.30	0.31	0.30	0.30	0.30	0.27	
Elongation at break, %	453.33 ± 10.33	446.67 ± 10.33	450.00 ± 10.95	453.33 ± 10.33	455.00 ± 8.37	455.00 ± 8.37	0.652
CV, %	2.28	2.31	2.43	2.28	1.84	1.84	
Δ95, %	2.39	2.43	2.55	2.39	1.93	1.93	
Tear resistance, kN/m	83.50 ± 2.43	81.90 ± 1.73	82.53 ± 1.11	83.00 ± 1.83	84.30 ± 2.36	83.00 ± 0.29	0.305
CV, %	2.91	2.12	1.35	2.21	2.79	0.35	
Δ95, %	3.05	2.22	1.41	2.31	2.93	0.37	
Shore A hardness, cond. un.	59.00 ± 1.41	59.00 ± 1.41	60.00 ± 1.41	60.00 ± 1.41	61.00 ± 1.79	59.00 ± 1.41	0.139
CV, %	2.40	2.40	2.36	2.36	2.93	2.40	
Δ95, %	2.52	2.52	2.47	2.47	3.08	2.52	
Bond strength of rubber with brass-coated steel cordmetal cord, N	301.17 ± 0.98	295.00 ± 0.63	299.00 ± 0.63	303.00 ± 0.63	305.00 ± 0.63	304.00 ± 0.63	<0.001
CV, %	0.33	0.21	0.21	0.21	0.21	0.21	
Δ95, %	0.34	0.22	0.22	0.22	0.22	0.22	

Note: Mean ± SD (n = 6); CV = SD/mean × 100%; Δ95 = relative half-width of the 95% confidence interval; ANOVA p-values refer to differences among the formulations within the series. CV and Δ95 values are reported to two decimal places; for values below 0.05%, three decimal places are retained.

Table 8. Physicomechanical properties of vulcanizates containing ZMN and statistical evaluation of test results.

Name of Indicators	Standard	Weight Parts 100 Pts.Wt Rubber					ANOVA, *p*
		1	2	3	4	5	
Conventional tension at 300% elongation, MPa	14.52 ± 0.033	14.34 ± 0.029	14.37 ± 0.052	14.52 ± 0.028	14.67 ± 0.004	14.50 ± 0.014	<0.001
CV, %	0.23	0.20	0.36	0.19	0.028	0.10	
Δ95, %	0.24	0.21	0.38	0.20	0.029	0.10	
Conventional tensile strength, MPa	20.02 ± 0.014	19.59 ± 0.014	19.62 ± 0.014	20.22 ± 0.014	20.33 ± 0.016	20.19 ± 0.014	<0.001
CV, %	0.07	0.07	0.07	0.07	0.08	0.07	
Δ95, %	0.07	0,08	0.08	0.07	0.08	0.07	

Table 8. *Cont.*

Name of Indicators	Standard	Weight Parts 100 Pts.Wt Rubber					ANOVA, *p*
		1	2	3	4	5	
Elongation at break, %	450.00 ± 10.95	446.67 ± 10.33	450.00 ± 10.95	454.00 ± 1.41	453.00 ± 1.41	445.00 ± 1.41	0.315
CV, %	2.43	2.31	2.43	0.31	0.31	0.32	
Δ95, %	2.55	2.43	2.55	0.33	0.33	0.33	
Tear resistance, kN/m	81.70 ± 0.14	79.20 ± 0.14	80.50 ± 0.19	81.30 ± 0.20	82.62 ± 0.27	79.20 ± 0.19	<0.001
CV, %	0.17	0.18	0.24	0.25	0.33	0.24	
Δ95, %	0.18	0.19	0.25	0.26	0.34	0.25	
Shore A hardness, cond. un.	60.00 ± 0.38	58.00 ± 0.40	59.00 ± 0.40	59.00 ± 0.33	62.00 ± 0.34	59.00 ± 0.28	<0.001
CV, %	0.63	0.69	0.68	0.56	0.55	0.48	
Δ95, %	0.66	0.72	0.71	0.58	0.58	0.50	
Bond strength of rubber with brass-coated steel cordmetal cord, N	295.00 ± 1.90	305.00 ± 1.90	308.00 ± 2.45	309.00 ± 2.45	310.00 ± 2.45	309.00 ± 1.90	<0.001
CV, %	0.64	0.62	0.80	0.79	0.79	0.61	
Δ95, %	0.67	0.65	0.83	0.83	0.83	0.64	

Note: Mean ± SD (n = 6); CV = SD/mean × 100%; Δ95 = relative half-width of the 95% confidence interval; ANOVA p-values refer to differences among the formulations within the series. CV and Δ95 values are reported to two decimal places; for values below 0.05%, three decimal places are retained.

Elongation at break (446.67–455.00% for ZMC and 445.00–454.00% for ZMN) did not differ significantly from the reference values (ANOVA $p = 0.652$ and 0.315, respectively), i.e., the elasticity of the vulcanizates was maintained.

Tensile strength depended on the dosage of the modified zeolite. At 6.0 and 7.0 phr it was lower than that of the reference compounds (19.80 and 20.10 MPa for ZMC; 19.59 and 19.62 MPa for ZMN), whereas at 8.0–9.12 phr it was comparable to or slightly higher than the reference values (up to 20.39 MPa for ZMC and 20.33 MPa for ZMN, versus 20.32 and 20.02 MPa for the references). At 10.0 phr the tensile strength was 20.21 and 20.19 MPa, i.e., there was no further increase. A similar dependence was observed for the conventional stress at 300% elongation (14.25–14.78 MPa for ZMC and 14.34–14.67 MPa for ZMN; references 14.71 and 14.52 MPa).

The tear resistance of the ZMC compounds (81.90–84.30 kN/m) did not differ significantly from that of the reference (83.50 kN/m; $p = 0.305$). For the ZMN compounds (79.20–82.62 kN/m) the differences were significant ($p < 0.001$): the highest value (82.62 kN/m) was obtained at 9.12 phr, whereas the other formulations were at or below the reference value (81.70 kN/m). Shore A hardness changed only slightly (58–62 conventional units), so no excessive increase in stiffness was observed.

All physical and mechanical parameters were determined on six replicate specimens, and the values in Tables 7 and 8 are the means of the parallel determinations. The highest strength was observed at 9.12 phr; a further increase in the modified zeolite content to 10.0 phr did not lead to a further increase in these parameters. The high elongation at break and the small change in hardness indicate that the strength was not achieved at the expense of elasticity.

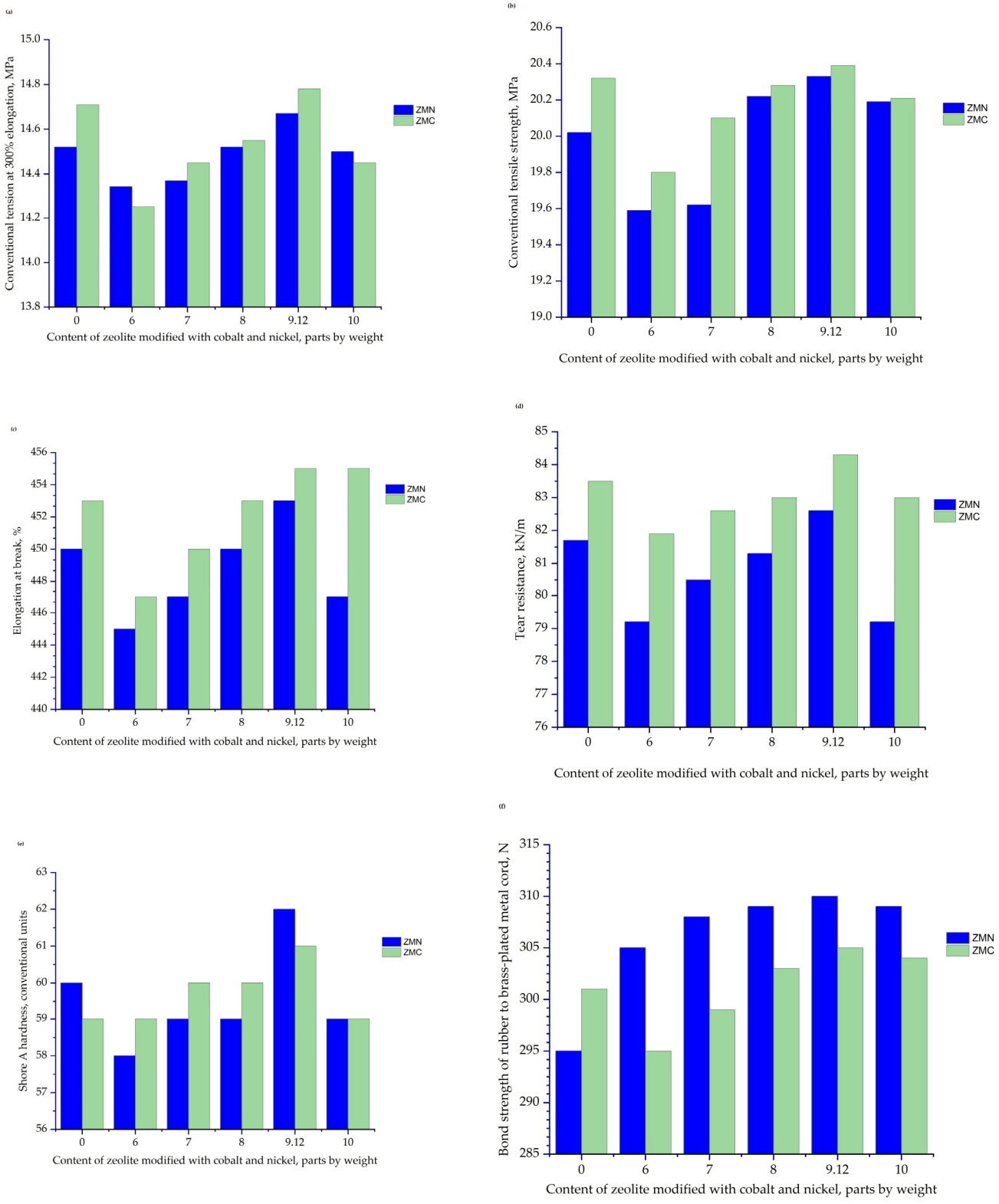


Figure 11. Physical and mechanical properties of vulcanizates and dosage of adhesion promoters: (**a**) conventional tension at 300% elongation, MPa; (**b**) conventional tensile strength, MPa; (**c**) elongation at break, %; (**d**) tear resistance, kN/m; (**e**) Shore A hardness, cond. un.; (**f**) bond strength of rubber with brass-coated steel cord metal cord, N.

A comparison of the physicomechanical and adhesive properties indicates that ZMC and ZMN affect the performance characteristics of the rubber compounds to different extents. Upon complete replacement of the conventional adhesion promoters with 9.12 phr

of modified zeolite, the tensile strength reaches 20.39 MPa for ZMC and 20.33 MPa for ZMN, compared with 20.32 and 20.02 MPa for the respective reference compounds. Thus, the increases in tensile strength are relatively modest, amounting to approximately 0.34% and 1.55%, respectively. In contrast, the rubber-to-brass-plated steel cord bond strength increases from 301.17 to 305.00 N for ZMC and from 295.00 to 310.00 N for ZMN, corresponding to improvements of approximately 1.27% and 5.08%, respectively. Therefore, the effect of the modified zeolites on adhesive performance is more pronounced than their effect on tensile strength, particularly in the ZMN-containing system.

These findings suggest that the action of ZMC and ZMN may not be limited to changes in the bulk physicomechanical properties of the vulcanizates but may also involve processes occurring during the formation of the rubber–metal interfacial region. Nevertheless, direct characterization of the chemical composition and structure of the interfacial layer is required to confirm this interpretation.

The adhesion tests showed that the bond strength between rubber and brass-plated steel cord depended on the dosage of the modified zeolites. For formulations 1–5, the measured bond strength ranged from 295 to 305 N for ZMC-containing compounds and from 305 to 310 N for ZMN-containing compounds, compared with 301.17 ± 0.98 N and 295.00 ± 1.90 N for the respective reference compounds (Tables 7 and 8). At a modified zeolite loading of 9.12 phr, the mean bond strengths were 305.00 ± 0.63 N for ZMC and 310.00 ± 2.45 N for ZMN (mean ± SD, n = 6). Although ZMN exhibited a slightly higher mean value, the difference of about 5 N (≈1.6%) is small, and the two systems were not compared statistically.

The mechanisms responsible for the observed adhesion behavior remain to be established. Based on previous studies of rubber–brass adhesion and of the role of transition-metal species in sulfur vulcanization [45–54], and on the results obtained in the present work, several possible contributions may be considered, including changes in vulcanization behavior, the availability of sulfur-containing species, and interactions involving the modified zeolite particles. However, these possibilities should be regarded as working hypotheses rather than experimentally demonstrated interfacial processes.

The formation of copper sulfide species at the rubber–brass interface has been reported in the literature. In particular, Ozawa et al. [47] investigated the chemical structure of the rubber–brass adhesive interface and identified the importance of copper sulfides in adhesion development. On this basis, it may be hypothesized that ZMC and ZMN influence the conditions under which the interfacial layer develops during vulcanization. Nevertheless, the chemical composition, thickness, and spatial distribution of the interfacial products were not determined in the present study.

The EDS results indicated cobalt and nickel contents of 2.6 wt.% in ZMC and 1.0 wt.% in ZMN, respectively. These values are semi-quantitative and do not distinguish between metal species located on external particle surfaces and those associated with the internal pore structure. Furthermore, the available XPS spectra do not permit oxidation-state assignments. Therefore, the observed differences in adhesion cannot be attributed to specific coordination interactions or to the formation of cobalt- or nickel-containing sulfide phases.

The role of the zeolite framework itself should also be considered. In the formulations studied here (Tables 3 and 4), the replacement of cobalt or nickel naphthenate by ZMC or ZMN simultaneously increases the content of the mineral component, and compounds containing unmodified zeolite under identical conditions were not prepared. Consequently, the individual contributions of the aluminosilicate framework and of the incorporated metal species cannot be separated.

The proposed interpretation is illustrated schematically in Figure 12. The diagram presents possible influences of ZMC and ZMN on the rubber–brass adhesive interface, rather

than a directly observed interfacial structure; the proposed effects on sulfur-containing species and interfacial layer development remain hypothetical.

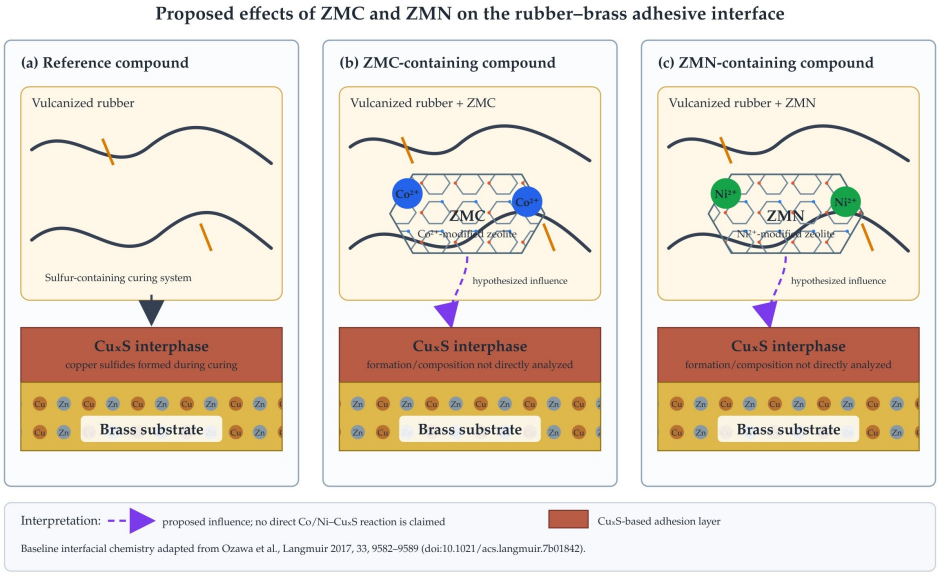


Figure 12. Proposed mechanisms of the influence of (**a**) the reference rubber compound, (**b**) ZMC, and (**c**) ZMN on the rubber–brass adhesive interface. The formation of a copper sulfide interphase, Cu_xS, during vulcanization is based on the experimentally established mechanism of rubber–brass adhesion reported by Ozawa et al. [47]. The effects of Co^{2+}- and Ni^{2+}-modified Chankanay zeolites are presented separately as mechanistic hypotheses based on the adhesion and curing results obtained in the present study. Dashed arrows indicate proposed rather than directly identified chemical interactions.

No microscopic or spectroscopic characterization of the extracted steel-cord surfaces or of the fracture surfaces after adhesion testing was performed. Consequently, the percentage of rubber coverage on the extracted cord was not determined, and no quantitative assessment of rubber coverage according to ASTM D2229 is reported. Further investigations, including rubber-coverage assessment after cord extraction and surface-sensitive characterization of the exposed interfaces (e.g., XPS and SEM–EDS), are required to clarify the adhesion mechanism and verify the proposed model.

The absence of a further increase in bond strength at ZMC or ZMN contents above 9.12 phr (304 and 309 N at 10.0 phr versus 305 and 310 N at 9.12 phr, i.e., within the scatter) may be associated with several factors. At excessive concentrations, an increased number of active sites and zeolite particles in the interfacial region may alter the organization and mechanical characteristics of the interfacial layer. In addition, partial shielding of the brass-coated steel cord surface and agglomeration of zeolite particles may reduce the effectiveness of interfacial interactions. Furthermore, increased adsorption of sulfur-containing species and accelerators on the zeolite surface at higher dosages may reduce their availability near the interface and thereby affect the formation of sulfide phases [45,49,51–55].

The resistance of rubbers to aging at elevated temperatures and exposure to aggressive environments is important because it ensures the stability of their structure and properties, reduces the rate of degradation processes, and, consequently, increases the reliability and service life of rubber products.

In the study of the resistance of vulcanizates containing the new adhesion promoters ZMC and ZMN to elevated temperature (100 °C), heat aging, and salt aging (Table 9), the formulations containing 9.12 parts by weight of ZMC and ZMN showed the most favorable performance. Compared with the corresponding formulations containing cobalt and nickel

naphthenates, respectively, the bond strength increased by 18% and 14.9% at 100 °C, by 9.8% and 11.9% after heat aging, and by 3.7% and 1.8% after salt aging.

Table 9. Bond strength of SKI-3-based rubber compounds to brass-plated steel cord under different exposure conditions.

Adhesion Promoter	Dosage of Adhesion Promoter, Parts by Weight	Bond Strength of Rubber to Brass-Plated Steel Cord, N			
		20 °C	100 °C	Thermal Aging (1)	Salt Aging (2)
Cobalt naphthenate	9.12	301	178	205	270
ZMC	7.0	299	198	210	250
	8.0	303	205	217	260
	9.12	305	210	225	280
Nickel naphthenate	9.12	295	195	210	285
ZMN	7.0	308	201	220	270
	8.0	309	215	230	280
	9.12	310	224	235	290

Notes under Table 9: (1) air at 120 °C for 16 h; (2) boiling in a 5% NaCl solution for 6 h.

A comparison of the results obtained at elevated temperature and after aging demonstrates that the advantages of the modified zeolites depend on the exposure conditions. At 100 °C, the bond strength of the ZMC-containing system reaches 210 N compared with 178 N for the reference compound, while the corresponding values for the ZMN-containing system are 224 and 195 N. After thermal aging, the bond strengths are 225 and 205 N for the cobalt-containing systems and 235 and 210 N for the nickel-containing systems, respectively. These results indicate that complete replacement of the naphthenate-based promoters with modified zeolites can maintain or improve the absolute adhesive bond strength under the investigated exposure conditions. However, the present data do not establish the specific mechanisms responsible for the improved high-temperature performance. The possible influence of modified zeolites on the formation and evolution of the interfacial layer requires further investigation.

The higher bond strength of the ZMC- and ZMN-containing compounds at 100 °C and after aging may be related to a more stable vulcanizate structure, a different course of the interfacial reactions, or a lower rate of thermo-oxidative degradation. These explanations are hypothetical, because the vulcanization network, the interfacial layer, and the degradation processes were not studied directly and compounds with unmodified zeolite were not tested.

Thus, based on the experimental data obtained, it can be concluded that zeolites modified with cobalt and nickel cations have the potential to be used as standalone adhesion promoters in rubber-metal systems. These results provide further insight into the functional capabilities of modified zeolites and indicate their potential application in elastomeric composite materials.

The use of ZMC and ZMN as adhesion promoters differs from that of traditional adhesion promoters. When modified zeolites are introduced into a rubber matrix, the potential toxicity of the system is determined not only by the nature of the metals (Co and Ni) but also by their form. In this case, the metal ions are immobilized within the zeolite structure and additionally retained in the polymer matrix, which may limit their mobility and the risk of their migration into the environment. Therefore, the results of this study do not allow definitive conclusions regarding the environmental safety of ZMC and ZMN. However, the method of fixing metal ions within the zeolite structure and polymer matrix is of interest for further study of their migration capacity. Evaluation of this aspect requires

specialized studies, including metal leaching and migration tests, as well as a toxicological assessment of the resulting materials.

4. Conclusions

The results of the study of the physical, mechanical, and adhesive properties of vulcanizates show that breaker rubber compounds containing zeolites modified with Co^{2+} and Ni^{2+} cations, at the optimal loading of 9.12 phr (complete replacement of the naphthenate), exhibit strength properties comparable to those of the reference compounds containing cobalt or nickel naphthenate, together with a slightly higher bond strength to brass-plated steel cord (305 N for ZMC and 310 N for ZMN versus 301 and 295 N for the respective references). At 100 °C, the bond strength was 18.0% (ZMC) and 14.9% (ZMN) higher than that of the reference compounds. These results indicate that modified zeolites are a promising alternative to conventional naphthenate adhesion promoters in rubber compounds for breaker products.

The use of zeolite from the Chankanay deposit as a basis for such promoters may be of practical interest, since it allows for the use of readily available natural mineral raw materials and may reduce the consumption of cobalt and nickel naphthenates. However, the metal contents were determined only semi-quantitatively by EDS, and the economic feasibility and environmental aspects, including process costs, material stability, and the migration and leaching of metal components, require further comprehensive assessment.

Because unmodified-zeolite controls were not included, the individual contributions of the aluminosilicate framework and of the incorporated Co and Ni species to the observed effects cannot be distinguished. Therefore, the obtained results should be viewed primarily as experimental evidence of the potential of modified zeolites in adhesive systems for breaker rubber.

Supplementary Materials: The following supporting information can be downloaded at: https://www.mdpi.com/article/10.3390/pr14233829/s1. Table S1. Individual measurements of physicomechanical properties of vulcanizates containing ZMC (n = 6 per formulation). Table S2. Individual measurements of physicomechanical properties of vulcanizates containing ZMN (n = 6 per formulation).

Author Contributions: Conceptualization, A.T. and Z.A.; methodology, A.S. (Aliya Suigenbayeva); software, A.T., M.N. and S.K.; validation, A.T., M.N. and A.S. (Abdujalol Sidikov); formal analysis, A.O.; investigation, A.O. and S.K.; resources, A.O.; data curation, A.O. and Z.A.; writing—original draft preparation, G.S.; writing—review and editing, G.S.; visualization, S.S. and A.S. (Aliya Suigenbayeva); supervision, S.S. and A.S. (Abdujalol Sidikov); project administration, A.O.; funding acquisition, A.S. (Aliya Suigenbayeva). All authors have read and agreed to the published version of the manuscript.

Funding: This research received no external funding.

Data Availability Statement: The original contributions presented in this study are included in the article/Supplementary Material. Further inquiries can be directed to the corresponding authors.

Conflicts of Interest: The authors declare no conflicts of interest.

References

1. Popa, C.M.; Gebhardt, C.; Raje, N.; Steenwyk, B.; Kaliske, M. Investigation of cord–rubber composite durability by the material force method. *Eng. Fract. Mech.* **2020**, *229*, 106909. [CrossRef]
2. Wu, Y.; Wu, J.; Su, B.; Teng, F.; Wang, Y. Study on the interface failure mechanism for cord/rubber composites of aircraft tire. *Polym. Compos.* **2026**, *47*, 4804–4818. [CrossRef]
3. Kutlubay, R.C.; Sekercioglu, T. Investigation of the factors affecting the strength of a metal–rubber interface joined by vulcanization: A review. *Mater. Tehnol.* **2024**, *58*, 683–698. [CrossRef]
4. Karmanova, O.V.; Tikhomirov, S.G.; Lintsova, E.V.; Popova, L.V. Research of the properties of rubber-cord composites in the presence of new adhesion promoters. *Proc. VSUET* **2020**, *82*, 221–226. (In Russian) [CrossRef]

5. Miyata, T.; Shimizu, K.; Sato, Y.K.; Jinnai, H. Atomic-scale analysis on a rubber–brass adhesive interface using scanning transmission electron microscopy. *Polymer* **2023**, *265*, 125602. [CrossRef]
6. Kasperovich, A.V.; Krotova, O.A.; Potapov, E.E.; Reznichenko, S.V.; Shkodich, V.F. A study of the influence of a new promoter on the adhesion of rubber to a metal cord. *Polym. Sci. Ser. D* **2016**, *9*, 68–71. [CrossRef]
7. Darwish, N.A.; Shehata, A.B.; Abou-Kandil, A.I.; Abd El-Megeed, A.A.; Lawandy, S.N.; Saleh, B.K. A novel promoter for enhancing adhesion between natural rubber and brass-plated steel cords. *Int. J. Adhes. Adhes.* **2013**, *40*, 135–144. [CrossRef]
8. Krotova, O.A.; Kasperovich, A.V.; Shashok, Z.S.; Stoyanov, O.V. Modified silica filler as a promoting agent of adhesion of rubber to metal cord. *Polym. Sci. Ser. D* **2018**, *11*, 1–5. [CrossRef]
9. Shi, X.; Ma, M.; Lian, C.; Zhu, D. Investigation of the effects of adhesion promoters on the adhesion properties of rubber/steel cord by a new testing technique. *J. Appl. Polym. Sci.* **2014**, *131*, 39460. [CrossRef]
10. Puchkov, A.F.; Turenko, S.V.; Kablov, V.F.; Titov, N.V. Adhesion Activating Agent of Rubbers to Brass-Coated Metal. Patent RU 2380385 C2, 27 January 2010. Available online: https://patents.google.com/patent/RU2380385C2/en (accessed on 17 November 2026).
11. Gehling, T.; Schieppati, J.; Balasooriya, W.; Kerschbaumer, R.C.; Pinter, G. Fatigue behavior of elastomeric components: A review of the key factors of rubber formulation, manufacturing, and service conditions. *Polym. Rev.* **2023**, *63*, 763–804. [CrossRef]
12. Sato, Y.K.; Miyata, T.; Shimizu, K. Nanoscale distribution and role of cobalt at the interface between brass-coated steel wire and rubber. *Rubber Chem. Technol.* **2026**, *99*, 226–238. [CrossRef]
13. Chen, X.; Zhang, T.; Sun, P.; Yu, F.; Li, B.; Dun, L. Application of organic amine modified natural zeolite in filling natural rubber. *Nanomaterials* **2022**, *12*, 2784. [CrossRef] [PubMed]
14. Orazymbetova, A.O.; Sagitova, G.F.; Sidikov, A.S.; Sakibaeva, S.A.; Issa, A.B. Applications of zeolites in various fields (review) [*Seolitterdiñ är türli salalarda qoldanu mümkındıkterı (şolu)*]. *Bull. Shakarim Univ. Tech. Sci.* **2025**, *1*, 376–397. [CrossRef] [PubMed]
15. Orazimbetova, A.O.; Sakibaeva, S.A.; Sagitova, G.F.; Suigenbaeva, A.Z. Study of physicochemical properties of zeolites in the Shankanai field [Shankanai ken ornyndagy zeolitterdine physics-chemistry kasietterin zertteu]. *News Natl. Acad. Sci. Repub. Kazakhstan Ser. Chem. Technol.* **2024**, *2*, 138–150. [CrossRef]
16. Orazimbetova, A.O.; Sagitova, G.F.; Sidikov, A.S.; Sakibaeva, S.A.; Suigenbaeva, A.Z. Physical and Chemical Modification of Natural Mineral of Chankanay Deposit [*Şanqanai ken ornyndağy seolitterdiñ fizika-himialyq qasietterın zertteu*]. *Bull. Shakarim Univ. Tech. Sci.* **2025**, *2*, 459–469. [CrossRef] [PubMed]
17. Orazymbetova, A.O.; Sagitova, G.F.; Sakibaeva, S.A.; Suigenbaeva, A.Z.; Jakipbekova, N.O.; Shingisbayeva, Z.A.; Issa, A.B.; Ashitova, N.Z. Method for Obtaining an Adhesion Promoter for Bonding Rubbers to Metals [*Sposob polucheniya promotora adgezii dlya krepleniya rezin k metallam*]. Patent of the Republic of Kazakhstan for Utility Model No. 10648, Application No. 2025/0385.2, 27 June 2025. Available online: https://gosreestr.kazpatent.kz/Gosreestr/DownloadDescription?documentId=3551963 (accessed on 1 July 2026).
18. Sagitova, G.; Khassankhojayeva, B.-M.; Takibayeva, G.; Kabylbekova, A.; Tileuberdi, A.; Daurenbek, N. Development of natural zeolite-based rubber compounds for water sealing applications. *Eng. Technol. Appl. Sci. Res.* **2026**, *16*, 36352–36360. [CrossRef]
19. Tsitsishvili, V.; Panayotova, M.; Mirdzveli, N.; Dzhakipbekova, N.; Panayotov, V.; Dolaberidze, N.; Nijaradze, M. Acid resistance and ion-exchange capacity of natural mixtures of heulandite and chabazite. *Minerals* **2023**, *13*, 364. [CrossRef]
20. Tsitsishvili, V.; Dolaberidze, N.; Mirdzveli, N.; Nijaradze, M.; Dzhakipbekova, N.; Harutyunyan, L.; Amiridze, Z.; Khutsishvili, B. Acid treatment of Georgian, Kazakhstani and Armenian natural heulandite-clinoptilolites II. Adsorption and porous structure. *InterConf+* **2023**, *147*, 483–502. [CrossRef]
21. Sagitova, G.; Khassankhojayeva, B.-M.; Tileuberdi, A.; Sidikov, A.; Daurenbek, N.; Takibayeva, G.; Kabylbekova, A. Oil-sludge valorization through organic-fraction recovery and its use as a substitute for petroleum processing oil in SKI-3 rubber compounds. *Processes* **2026**, *14*, 3058. [CrossRef]
22. *Standard GOST 415-75*; Rubber and Rubber Mixes—Method for Determination of Plasticity by Means of Plastometer. Standards Publishing House: Moscow, Russia, 1975.
23. *Standard GOST 12535-84*; Raw Rubber—Method for Determination of Curing Characteristics by Curemeter. Standards Publishing House: Moscow, Russia, 1984.
24. *Standard GOST R 54553-2019*; Rubber and Thermoplastic Elastomers—Determination of Tensile Stress–Strain Properties. Standartinform: Moscow, Russia, 2019.
25. *Standard GOST 262-93 (ISO 34-79)*; Rubber—Determination of Tear Strength (Trouser, Angle and Crescent Test Pieces). Standards Publishing House: Moscow, Russia. Available online: https://allgosts.ru/83/060/gost_262-93 (accessed on 21 November 2026).
26. *Standard GOST 263-75*; Rubber—Method for Determination of Shore A Hardness. Standards Publishing House: Moscow, Russia. Available online: https://allgosts.ru/83/060/gost_263-75 (accessed on 21 November 2026).
27. *Standard GOST ISO 5603-2013*; Rubber—Determination of Adhesion to Wire Cord. Standartinform: Moscow, Russia, 2014.
28. Li, M.; Zhu, X.; Zhu, F.; Ren, G.; Cao, G.; Song, L. Application of modified zeolite for ammonium removal from drinking water. *Desalination* **2011**, *271*, 295–300. [CrossRef]

29. Dávila-Jiménez, M.M.; Elizalde-González, M.P.; Mattusch, J.; Morgenstern, P.; Pérez-Cruz, M.A.; Reyes-Ortega, Y.; Wennrich, R.; Yee-Madeira, H. In situ and ex situ study of the enhanced modification with iron of clinoptilolite-rich zeolitic tuff for arsenic sorption from aqueous solutions. *J. Colloid Interface Sci.* **2008**, *322*, 527–536. [CrossRef] [PubMed]
30. Tattibayeva, Z.A.; Tursynbetov, M.T.; Tazhibayeva, S.M.; Kujawski, W.; Musabekov, K.B. Adsorption modification of the zeolite surface with chitosan. *Chem. Bull. Kaz. Natl. Univ.* **2019**, *95*, 20–26. [CrossRef]
31. Rodríguez-Iznaga, I.; Costa Marrero, Y.; Farias Piñeira, T.; Fontaine, C.; Paget, L.; Concepción Rosabal, B.; Penton Madrigal, A.; Petranovskii, V.; Lafaye, G. Zeolite materials with Ni and Co: Synthesis and catalytic potential in the selective hydrogenation of citral. *Beilstein J. Nanotechnol.* **2025**, *16*, 520–529. [CrossRef] [PubMed]
32. Belova, T.P. Adsorption of heavy metal ions (Cu^{2+}, Ni^{2+}, Co^{2+} and Fe^{2+}) from aqueous solutions by natural zeolite. *Heliyon* **2019**, *5*, e02320. [CrossRef] [PubMed]
33. Munthali, M.W.; Elsheikh, M.A.; Johan, E.; Matsue, N. Proton adsorption selectivity of zeolites in aqueous media: Effect of Si/Al ratio of zeolites. *Molecules* **2014**, *19*, 20468–20481. [CrossRef] [PubMed]
34. Baer, D.R.; Artyushkova, K.; Brundle, C.R.; Castle, J.E.; Engelhard, M.H.; Gaskell, K.J.; Grant, J.T.; Haasch, R.T.; Linford, M.R.; Powell, C.J.; et al. Practical guides for X-ray photoelectron spectroscopy: First steps in planning, conducting, and reporting XPS measurements. *J. Vac. Sci. Technol. A* **2019**, *37*, 031401. [CrossRef] [PubMed]
35. Kaushik, V.K.; Vijayalakshmi, R.P.; Choudary, N.V.; Bhat, S.G.T. XPS studies on cation exchanged zeolite A. *Microporous Mesoporous Mater.* **2002**, *51*, 139–144. [CrossRef]
36. Bare, S.R.; Knop-Gericke, A.; Teschner, D.; Hävecker, M.; Blume, R.; Rocha, T.C.R.; Schlögl, R.; Chan, A.S.Y.; Blackwell, N.; Charochak, M.E.; et al. Surface analysis of zeolites: An XPS, variable kinetic energy XPS, and low energy ion scattering study. *Surf. Sci.* **2016**, *648*, 376–382. [CrossRef]
37. Chen, X.; Shen, B.-X.; Sun, H.; Zhan, G.-X. Ion-exchanged zeolites Y for selective adsorption of methyl mercaptan from natural gas: Experimental performance evaluation and computational mechanism explorations. *Ind. Eng. Chem. Res.* **2017**, *56*, 10164–10173. [CrossRef]
38. Olszewska, D. Application of XPS method in the research into Ni ion-modified montmorillonite as a SO_2 sorbent. *Fuel Process. Technol.* **2012**, *95*, 90–95. [CrossRef]
39. Lemishka, M.; Dědeček, J.; Mlekodaj, K.; Sobalík, Z.; Sklenák, S.; Tabor, E. Speciation and Siting of Divalent Transition Metal Ions in Silicon-Rich Zeolites: An FTIR Study. *Pure Appl. Chem.* **2019**, *91*, 1721–1732. [CrossRef]
40. Sobalík, Z.; Tvarůžková, Z.; Wichterlová, B. Skeletal T–O–T Vibrations as a Tool for Characterization of Divalent Cation Complexation in Ferrierite. *J. Phys. Chem. B* **1998**, *102*, 1077–1085. [CrossRef]
41. Mozgawa, W.; Król, M.; Bajda, T. Application of IR spectra in the studies of heavy metal cations immobilization on natural sorbents. *J. Mol. Struct.* **2009**, *924–926*, 427–433. [CrossRef]
42. Stojanov, S.; Govedarica, O.; Milanović, M.; Žeravica, J.; Barta Holló, B.; Govedarica, D.; Jovičić, M. The Effect of Synthetic Zeolite on the Curing Process and the Properties of the Natural Rubber-Based Composites. *Polymers* **2024**, *16*, 3228. [CrossRef] [PubMed]
43. Milani, G.; Leroy, E.; Milani, F.; Deterre, R. Mechanistic Modeling of Reversion Phenomenon in Sulphur-Cured Natural Rubber Vulcanization Kinetics. *Polym. Test.* **2013**, *32*, 1052–1063. [CrossRef]
44. Bornstein, D.; Pazur, R.J. The Sulfur Reversion Process in Natural Rubber in Terms of Crosslink Density and Crosslink Density Distribution. *Polym. Test.* **2020**, *88*, 106524. [CrossRef]
45. Krotova, O.A.; Kasperovich, A.V.; Shashok, Z.S.; Stoyanov, O.V. Adhesive properties of rubbers with promoters based on modified silica filler. *Polym. Sci. Ser. D* **2017**, *10*, 128–133. [CrossRef]
46. Fulton, W.S.; Smith, G.C.; Titchener, K.J. Interfacial microanalysis of rubber–tyre-cord adhesion and the influence of cobalt. *Appl. Surf. Sci.* **2004**, *221*, 69–86. [CrossRef]
47. Ozawa, K.; Kakubo, T.; Amino, N.; Mase, K.; Ikenaga, E.; Nakamura, T. Angle-Resolved HAXPES Investigation on the Chemical Origin of Adhesion between Natural Rubber and Brass. *Langmuir* **2017**, *33*, 9582–9589. [CrossRef] [PubMed]
48. Mandal, N.; Sajith, P.; Agrawal, S.L.; Bandyopadhyay, S.; Mukhopadhyay, R.; D'Cruz, B. Synthesis of cobalt adhesion promoters and their evaluation in a passenger radial-belt skim compound. *J. Adhes.* **2005**, *81*, 911–923. [CrossRef]
49. Abou-Kandil, A.I.; Saleh, B.K.; Darwish, N.A. Rubber adhesion to metal surfaces with emphasis on rubber/brass adhesion: A critical review. *Rev. Adhes.* **2013**, *1*, 365–396. [CrossRef]
50. Souid, A.; Sarda, A.; Deterre, R.; Leroy, E. Rheological characterization and modelling of the rubber to metal vulcanization-bonding process. *Polym. Test.* **2014**, *36*, 88–94. [CrossRef]
51. Ling, C.Y.; Hirvi, J.T.; Suvanto, M.; Bazhenov, A.S.; Ajoviita, T.; Markkula, K.; Pakkanen, T.A. A computational study of adhesion between rubber and metal sulfides at the rubber–brass interface. *Chem. Phys.* **2015**, *453–454*, 7–12. [CrossRef]
52. Ashida, M.; Nakatani, M.; Takemoto, Y.; Goto, M. Studies on bonding rubber to metallic zinc (III): The effect of accelerators on adhesion of NR with cobalt salts to zinc plate. *Nippon Gomu Kyokaishi* **1984**, *57*, 544–552. [CrossRef]
53. Jeon, G.S. Enhancing the adhesion retention by controlling the structure of the adhesion interphase between rubber compound and metal. Part I: Effect of cobalt salt. *J. Adhes. Sci. Technol.* **2009**, *23*, 913–930. [CrossRef]

54. Ishikawa, Y. Adhesion of rubber to steel cord (1): Behaviors of adhesion build-up at the interface between rubber and brass plating of steel cord. *Nippon Gomu Kyokaishi* **2017**, *90*, 296–302. [CrossRef]
55. Jesmin, F.; Mitu, J.F.; Khandaker, T.; Ahmed, B.M.I.; Anik, M.A.A.M.; Anojaidi, K.I.; Al-Suwaylih, W.A.; Hasan, M.K.; Hossain, M.S. Recent advances in nanoparticle-modified zeolites: Functionalization strategies and diverse applications. *RSC Adv.* **2026**, *16*, 8828–8860. [CrossRef] [PubMed]

Disclaimer/Publisher's Note: The statements, opinions and data contained in all publications are solely those of the individual author(s) and contributor(s) and not of MDPI and/or the editor(s). MDPI and/or the editor(s) disclaim responsibility for any injury to people or property resulting from any ideas, methods, instructions or products referred to in the content.